Modified DMRG algorithm for the zigzag spin-1/2 chain with frustrated antiferromagnetic exchange: Comparison with field theory at large J_2/J_1

Manoranjan Kumar[1], Zoltán G. Soos[1], Diptiman Sen[2] and S. Ramasesha[3]
[1]*Department of Chemistry, Princeton University, Princeton NJ 08544*

[2]*Centre for High Energy Physics, Indian Institute of Science, Bangalore 560012, India and*
[3]Solid *State and Structural Chemistry Unit, Indian Institute of Science, Bangalore 560012, India*

(Dated: January 27, 2010)

A modified density matrix renormalization group (DMRG) algorithm is applied to the zigzag spin-1/2 chain with frustrated antiferromagnetic exchange J_1, J_2 between first and second neighbors. The modified algorithm yields accurate results up to $J_2/J_1 \approx 4$ for the magnetic gap Δ to the lowest triplet state, the amplitude B of the bond order wave (BOW) phase, the wavelength λ of the spiral phase, and the spin correlation length ξ. The J_2/J_1 dependences of Δ, B, λ and ξ provide multiple comparisons to field theories of the zigzag chain. The twist angle of the spiral phase and the spin structure factor yield additional comparisons between DMRG and field theory. Attention is given to the numerical accuracy required to obtain exponentially small gaps or exponentially long correlations near a quantum phase transition.

PACS numbers: 75.10.Jm, 75.10.Pq,75.40.Mg, 75.40.Cx
Email: soos@princeton.edu

I. INTRODUCTION

Extended one-dimensional (1D) models are excellent approximations for the electronic structure of some crystals, either inorganic or organic. Quite separately, 1D models have interesting theoretical and thermodynamic properties. In addition to exact results, approximate methods have been widely applied to and tested on 1D models. Two major recent developments are the density matrix renormalization group (DMRG) and field theory. The two methods are complementary in principle, and both have been applied to the zigzag spin-1/2 chain that is the subject of this paper. In practice, however, field theory deals with small energy gaps or long correlations lengths near quantum phase transitions that may be beyond the accuracy of numerical methods, a point often made for Kosterlitz-Thouless transitions. The two approaches to extended 1D systems are quite different. DMRG is a versatile numerical technique for growing an extended chain from a finite one. It provides a complete approximate description of the ground state (gs) or other properties. When multiple DMRG schemes are possible, the most accurate one is readily identified. Field theory is an analytical approach based on a continuum approximation, or an effective Hamiltonian, to a discrete 1D model. It targets critical phenomena at quantum phase transitions. A 1D model may support multiple field theories among which it may be difficult to choose.

In this paper, we present a modified DMRG algorithm to the zigzag spin-1/2 chain with frustrated antiferromagnetic (AF) exchange $J_1 > 0$ and $J_2 > 0$ between first and second neighbors. The Hamiltonian of this familiar 1D spin system is

$$H(x) = J \sum_n \; [(1-x)\vec{S}_n \cdot \vec{S}_{n+1} + x\vec{S}_n \cdot \vec{S}_{n+2}]. \qquad (1)$$

We consider the interval $0 \leq x \leq 1$ and set the total exchange $J = 1$ as the unit of energy. The $x = 0$ limit is a linear Heisenberg antiferromagnet (HAF) with many known exact properties [1] and many physical realizations. The $x \approx 1$ limit corresponds to two HAFs, one on each sublattice, and is the zigzag chain sketched in Fig. 1. Small J_1 for $x < 1$ or $x > 1$ describes an interchain exchange that is AF or ferromagnetic (F), respectively, and is frustrated because each spin is equally coupled to two neighbors of the other sublattice. The modified algorithm improves the accuracy for $x > 0.5$ ($J_2/J_1 > 1$).

The spin chain $H(x)$ has been extensively studied, especially in the $x = 0$ limit [1] that Bethe [2] and Hulthen [3] solved long ago. Majumdar and Ghosh (MG) found [4] a simple exact gs at $x_{MG} = 1/3$ ($J_2 = J_1/2$). The gs is a doubly degenerate bond order wave (BOW) with broken inversion symmetry at sites. The fluid-dimer transition with increasing J_2/J_1 marks the opening of a magnetic gap $\Delta(x)$ between the singlet gs and the lowest triplet state. The first field theoretic treatment [5] placed the critical ratio of J_2/J_1 at 1/3; subsequent analysis returned [6] $J_2/J_1 = 1/6$ and finally [7] $\approx 1/4$. Okamoto and Nomura [8] obtained the accepted value, $J_2/J_1 = 0.2411$ or $x_c = 0.1943$ in our notation, using

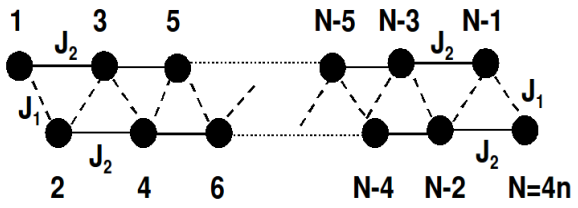

FIG. 1: Zigzag spin-1/2 chain with AF exchange J_1 and J_2 between first and second neighbors, respectively. $J_1 = 0$ gives two Heisenberg chains of $2n$ spins with exchange J_2

exact results up to $N = 24$ sites, extrapolation and field theory.

Classical spins in $H(x)$ lead to spiral phases for large J_2/J_1 when adjacent spins are nearly orthogonal. The gs energy per site for classical spins with angle θ between neighbors is

$$E_{cl}(\theta) = J_1 cos\theta + J_2 cos(2\theta). \tag{2}$$

Minimization with respect to θ leads to $cos\theta = -J_1/4J_2$ and $\theta = \pi/2 + \chi$ for large J_2/J_1. The spiral phases of quantum spins [9–11] are another area of interest, as are the structure factor [9] $S(q)$ as a function of J_2/J_1 and the crossover [12] from a singlet to a ferromagnetic gs at $J_1 = -4J_2$. There are possible physical realizations [13] of $H(x)$, most with AF exchanges J_1, J_2 and a few with F exchange J_1.

White and Affleck (WA) studied [14] the BOW phase with J_2/J_1 beyond the MG point by a combination of DMRG and field theory. Numerical issues limited DMRG to $J_2/J_1 = 2.0$ for Δ and to 2.5 for the order parameter. The modified algorithm is accurate up to $J_2/J_1 = 4$. WA concluded that the BOW phase extends to $x = 1$ ($J_1 = 0$). Itoi and Qin (IQ) presented [15] a more elaborate field theory for large J_2/J_1. The present work was motivated in part by the contrasting results of IQ and WA. According to IQ, the spin correlation length diverges as [15]

$$\xi(J_1, J_2) \approx exp(c(|J_1|/J_2)^{-2/3}), \tag{3}$$

where c is a constant. The WA expression [14] for ξ has exponent -1 instead of $-2/3$ and is limited to $J_1 > 0$. The order parameter of the BOW phase is

$$B(x) = \langle \vec{S}_n \cdot \vec{S}_{n+1} \rangle - \langle \vec{S}_n \cdot \vec{S}_{n-1} \rangle. \tag{4}$$

$B(x)$ is the gs amplitude of the BOW for $x > x_c$. WA call it "dimerization", a term that we reserve [16] for structurally dimerized systems such as polyacetylene or ion-radical salts or spin chains. Broken inversion symmetry in a BOW phase is *electronic* dimerization in a regular array. Both WA and IQ support their $\xi(x)$ with the same (limited) DMRG results [14] for $B(x)$ and $\Delta(x)$.

Since $B(x)$ and $\Delta(x)$ are proportional to $1/\xi(x)$, DMRG for the BOW amplitude or the magnetic gap can be compared to field theory as

$$lnB(x) \approx ln\Delta(x) \approx -c(J_1/J_2)^{-2/3} \tag{5}$$

with $J_2/J_1 = x/(1-x)$. The numerical problem is to evaluate exponentially small quantities at large J_2/J_1. The two computations are independent, since $\Delta(x)$ requires the triplet state while $B(x)$ does not. DMRG directly yields approximate spin correlations functions in the gs

$$C(p) = \langle \vec{S}_n \cdot \vec{S}_{n+p} \rangle, \tag{6}$$

and the wavelength $\lambda(x)$ of a spiral phase, if present. As noted by WA [14], $B(x)$ and $\Delta(x)$ are well-defined quantities whereas $\xi(x)$ requires an unknown fitting function in addition to $C(p)$. The order parameter of the spiral phase is the twist angle $\chi(x)$ below Eq. (2) that is related [11, 14] to the BOW phase as

$$\theta(x) - \frac{\pi}{2} = \chi(x) = \frac{\pi}{4\xi}. \tag{7}$$

$\chi(x) = 2\pi/\lambda(x)$ has been approximated by a coupled-cluster expansion [9] and by twisted boundary conditions in finite systems [11].

A spiral phase of $H(x)$ has been analyzed [10] in the classical limit of an infinite spin at each site in terms of a nonlinear σ-model that involves a 3×3 orthogonal matrix. That field theory does not produce a BOW, however, and is not powerful enough to yield scaling results for $\lambda(x)$ or $\Delta(x)$. On the other hand, field theories [14, 15] based on bosonization do not predict a parameter range in which a spiral phase should appear. Indeed, there is no compelling field theoretic reason that necessarily relates the spiral and BOW phase. They have different order parameters and different symmetries, a discrete symmetry for translation by one site in the BOW phase and a continuous rotational symmetry for the spiral phase. The BOW extends from [8] $x_c = 0.1943$ to [14] $x = 1$, while the range of a spiral phase is [17] from $x_{MG} = 1/3$ to $x = 1$. The richness of the zigzag chain at large J_2/J_1 makes it ideal for a critical discussion of DMRG accuracy and comparisons to field theory.

Section II describes the modified DMRG algorithm in which four rather than two spins are added per step. The accuracy improves modestly at $x = 0$ and dramatically for $x > 2/3$ where the second-neighbor J_2 dominates. Adding four spins when J_1 is small amounts to increasing two weakly-coupled chains by two spins each, just as adding two spins does at $x = 0$ in conventional DMRG. We present results in Section III for $B(x)$ and $\Delta(x)$ up to $x = 0.8$ ($J_2/J_1 = 4$) and for $\chi(x)$ and $\lambda(x)$ up to $x = 0.75$ ($J_2/J_1 = 3$), the practical limit in chains of $N < 1000$ spins with open boundary conditions (OBC). Our results agree with the IQ expression in Eq. (3) with $c = 2.90 \pm 0.10$ for all four quantities. We also compute the structure factor $S(q)$ and its maximum q^* that yields an independent estimate of the twist angle $\chi(x)$. We comment in Section IV on the status of comparisons between DMRG and field theory for the zigzag chain at large J_2/J_1.

II. MODIFIED DMRG ALGORITHM

DMRG is among the most accurate numerical techniques for solving extended 1D quantum cell models [18–21]. Conventional DMRG algorithms start with four sites and grow an extended chain by adding two sites in the middle, treating the left and right half-blocks as system and environment by turns [18, 19]. The accuracy of this method decreases for long-range (beyond first neighbor) interactions since we encounter bonds between old sites of the same system block. Long-range interactions in conventional DMRG couple sites at every step whose operators have undergone an unequal number of renormalizations. The spin chain $H(x)$ in Eq. (1) has second-neighbor J_2 between sites introduced on successive steps. The decrease in accuracy becomes significant when J_2 is large because site operators involved in J_2 are renormalized twice while the J_1 operators are renormalized only once. A remedy is to add sites on every step that encompass the full range of interactions.

Accordingly, we modified the DMRG algorithm for $H(x)$ to add two new sites per half block instead of one, as shown schematically in Fig. 2. The system starts with 4 spins and grows to $N = 4n$ in $N-1$ steps. Large J_2/J_1 leads to weakly coupled chains of $2n$ sites in Fig. 1, each with a singlet gs when $J_1 = 0$. The Fock space dimensionality of each block increases as $2(2s+1)m$, or as $4m$ for $s = 1/2$ sites, which is comparable to fermionic systems. We find that keeping $m = 150$ eigenvectors of the density matrix is sufficient for good accuracy. The truncation error in the sum of the eigenvalues of the density matrix is less than 10^{-9} in the worst case, and increasing m changes the energy only in 5^{th} or 6^{th} decimal place, in units of J. For more accurate spin correlation functions $C(p)$ and order parameter $B(x)$, we used finite DMRG calculations on every fourth steps [19]. $B(x)$ is calculated using the middle bonds of the chain and is accurate up to 5-6 decimal place, but is subject to finite-size effects of order $1/N$ discussed below.

We compare the modified algorithm with four sites added per step to conventional DMRG for the gs energy and the gap magnetic Δ. We use the infinite DMRG algorithm with $m = 200$ in each case. Since DMRG targets the lowest state in each M_S sector, the lowest permissible total spin state has the best energy in an AF model. Conventional DMRG is most accurate at $x = 0 (J_2 = 0)$ where there is only nearest-neighbor exchange. Nevertheless, as shown by the inset in Fig. 3, the new method improves the gs energy slightly and the triplet energy considerably. Note that the inset energy scale is 100 times finer that of the main figure. We attribute better performance to (i) the absence of old-old bonds within the same block in the new scheme, and (ii) increased number of new-new bonds (3 at $x = 0$) compared to new-old bonds (2 at $x = 0$) when four new sites are added at each step. The conventional ratio is 1:2 at $x = 0$. The accuracy of the new method at $x = 0$ is about 10^{-7} for the singlet and 10^{-5} for the triplet. It runs smoothly for

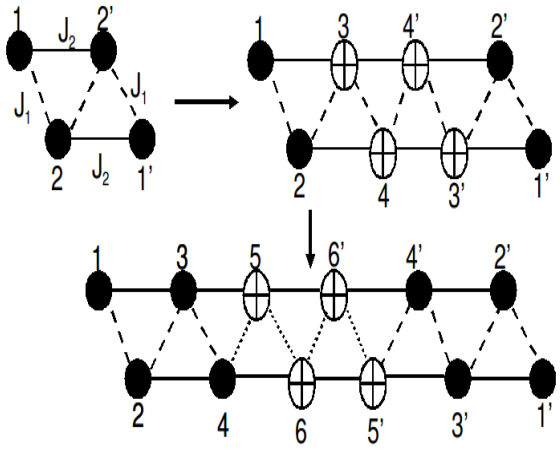

FIG. 2: DMRG scheme with four new sites added per step. Primed and unprimed indices are sites of the left and right blocks, respectively. Open circles represent new sites and closed circles, old sites. Solid lines represent J_2, dashed lines J_1.

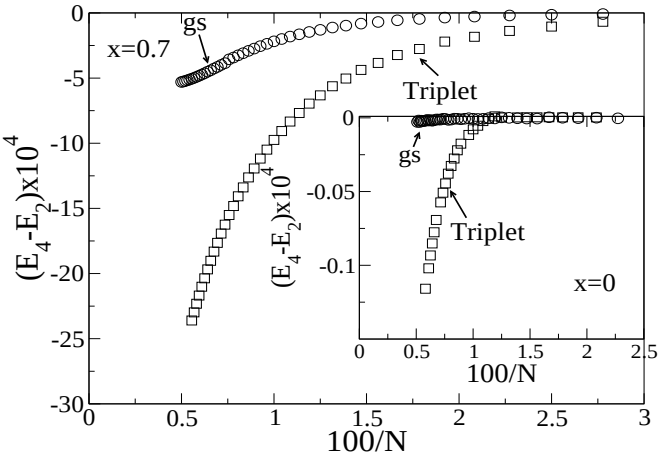

FIG. 3: Energy difference per site between the new (E_4) and conventional (E_2) DMRG for the singlet gs and the lowest triplet at $x = 0.70$ and $x = 0$ (inset) for chains of N sites.

$x > 2/3$, in contrast to numerical difficulties [14] of conventional DMRG at $x > 1/2$. The estimated accuracy for $x > 0.5$ is 10^{-5} for the gs and 10^{-3} for the triplet. We also studied chains with $J_2 > 0$ and F exchange $J_1 < 0$ in terms of J_1, J_2 rather than $x > 1$ in Eq. (1).

Figure 4 shows the size dependence of $B(0.8)$ and $\Delta(0.8)$ at $J_2/J_1 = 4.0$. These are the smallest B and Δ that are accurate with the present DMRG. We varied m to look for jumps in $B(x)$, such as those in Fig. 6 of ref. 14 at $J_2/J_1 = 2.5$, but found only the smooth

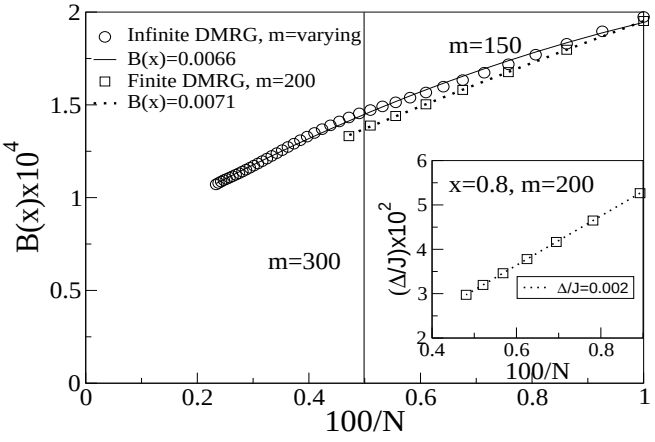

FIG. 4: BOW order parameter $B(0.80)$ vs $1/N$ for finite and infinite DMRG and (inset) magnetic gap $\Delta(0.80)$ vs $1/N$. Infinite DMRG is carried out with $m = 300$ for $N > 200$ and $m = 150$ for $N < 200$; finite DMRG has $m = 200$.

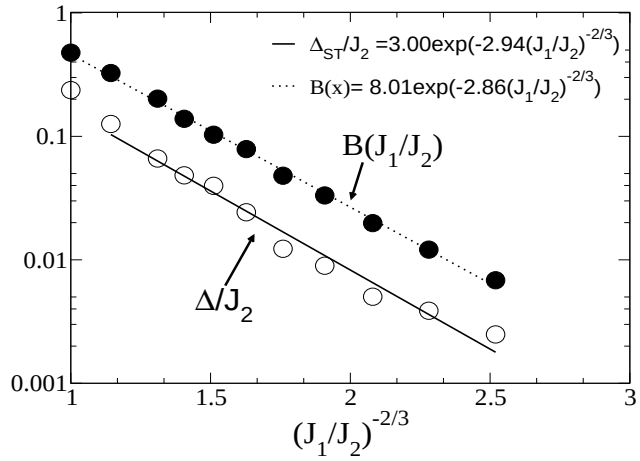

FIG. 5: Order parameter B and magnetic gap Δ as a function of $(J_1/J_2)^{-2/3}$. The fitted lines are $1/\xi(x)$ in Eq. (3) with $c = 2.94$ for Δ and 2.86 for B.

behavior shown. In the four-site algorithm, $B(x)$ is linear in $1/N$ for large N. Finite DMRG procedure with $m = 200$ and N between 100 and 200 sites returns $B(0.8) = 0.0071$, as shown in Fig. 4. The infinite algorithm with variable m, and $200 \leq N \leq 430$ leads to extrapolated $B(0.8) = 0.0066$. The inset of Fig. 4 shows the $1/N$ dependence of $\Delta(0.8)$ using finite DMRG with four spins added per step. The extrapolated gap is 0.002. Similar extrapolation at $x = 0$ give $\Delta \approx 0.001$, close to the exact $\Delta = 0$.

III. THE $J_2/J_1 > 1$ REGIME OF $H(x)$

Larger J_2/J_1 is accessible with the improved DMRG algorithm. All results below are for $m = 200$ and OBC for $N = 800$ sites, as discussed in Section II. The order parameter $B(x)$ in Eq. (4) and the magnetic gap $\Delta(x)$ from the gs to the lowest triplet provide direct comparison to field theory of the BOW phase. Both $B(x)$ and $\Delta(x)$ go as $1/\xi(x)$, where $\xi(x)$ is the correlation length in Eq. (3). As seen in Fig. 5, the IQ exponent of $-2/3$ fits the DMRG results remarkably well up to $J_2/J_1 = 4$ ($x = 0.8$) with $c = 2.90$. The $B(x)$ fit covers almost two orders of magnitude and extends to $J_2 = J_1$.

The $J_2/J_1 = 1$ point for Δ deviates upward from the line in Fig. 5. IQ used DMRG [14] for $\Delta(x)$ in the interval $0.6 \leq J_2/J_1 \leq 2$ to support ξ in Eq. (3) with $c = 3.66$. This is not correct, and the one-loop approximation does not extend down to $J_2/J_1 \approx 1$. WA used DMRG for $B(x)$ up to $J_2/J_1 = 2.5$ to support ξ with exponent -1 instead of $-2/3$ in Eq. (3). Their expression fails at larger J_2/J_1. DMRG with $0.6 \leq J_2/J_1 \leq 2.5$ is not appropriate for the BOW phase at large J_2/J_1. Although Fig. 5 covers more than an order of magnitude in Δ and almost two for B, there is no assurance that $J_2/J_1 = 4$ is large enough. On the other hand, if $J_2/J_1 \approx 4$ is not "large", numerical comparison with field theory will indeed be difficult.

The accuracy of $B(x)$ is limited by finite-size effects for OBC and $N = 800$ sites. We illustrate with an uncorrelated example. A half-filled Hückel or tight-binding chain of N sites has bond orders [22]

$$p_m = 2 \sum_{k=1}^{N/2} c_{k,m} c_{k,m+1}, \tag{8}$$

with $m = 1, 2, ..., N-1$. The coefficient $c_{k,m}$ at site m of the filled orbital k is

$$c_{k,m} = \sqrt{\frac{2}{N+1}} sin \frac{\pi k m}{N+1}. \tag{9}$$

The geometrical series for p_m is summed for finite N. The difference between $p_{N/2}$ of the central bond and that of either neighbor is $-2(-1)^{N/2}/N$ for large N. The bond order $p_{N/2}$ is less than the band limit of $2/\pi$ for $N = 4n$ and greater than $2/\pi$ for $N = 4n + 2$, just as expected for partial single and double bonds at the center of linear polyenes with evenly spaced C atoms. Since OBC break inversion symmetry at sites, this elementary example has implications for any OBC simulation of BOW systems. In any case, the exponential decrease of B with J_2/J_1 is soon overwhelmed by $1/N$ corrections that limit DMRG with $N \approx 1000$. Finite-size corrections to Δ or other low-energy excitations also go as $\approx 1/N$ and place similar limits on the accuracy of exponentially small gaps.

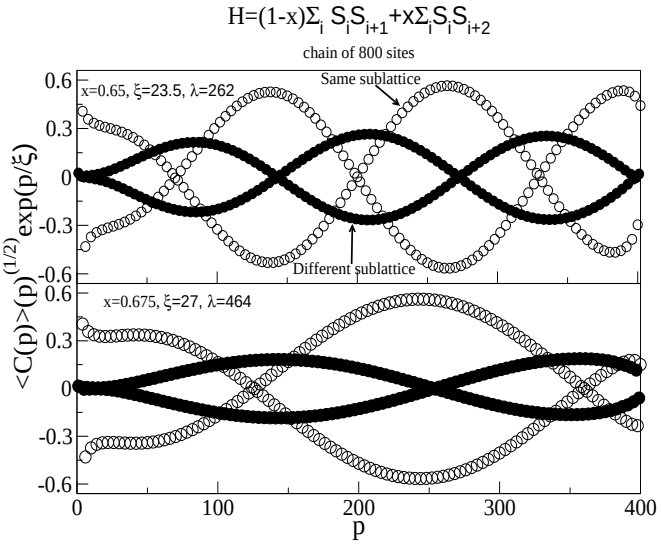

FIG. 6: Spin correlation functions $C(p)$ on the same sublattice (open symbols, even p) and on opposite sublattices (closed symbols, odd p) for $N = 800$ sites. The scaling of $C(p)$ and choice of are discussed in text.

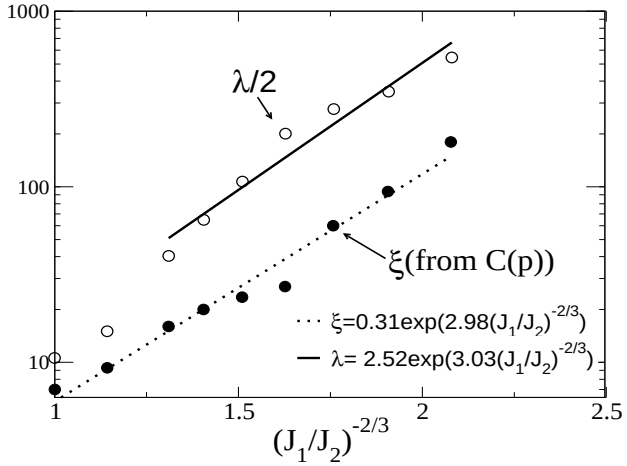

FIG. 7: Spin correlation length ξ of the BOW phase and the wavelength $\lambda(x)$ of the spiral phase as functions of $(J_1/J_2)^{-2/3}$, based on the $C(p)$ results on Fig. 6.

A DMRG calculation returns all gs spin correlations functions $C(p)$ in Eq. (6). OBC implies that $C(n,p)$ depends on the site index n as well as the separation p. It is customary to take sites n and $n+p$ in the central part of the chain. $C(p)$ between sites on one sublattice in Fig. 1 has even p, while $C(p)$ between sublattices has odd p. Fig. 6 shows $C(p)$ in spiral phases at $x = 0.65$ in the top panel and $x = 0.675$ in the bottom panel. The wavelength $\lambda(x)$ of the spiral phase appears directly provided that there are two nodes to specify $\lambda/2$. DMRG with $N = 800$ sites yields λ only up to $x = 0.75$. The scale factor $p^{1/2}exp(p/\xi)$ follows WA, who [14] considered even p and chose ξ to make the amplitudes in Fig. 6 as equal as possible. The same ξ holds for odd p. This procedure minimally requires two maxima and hence is also limited to $x = 0.75(J_2/J_1 = 3)$.

We obtained $\lambda(x)$ and $\xi(x)$ from $C(p)$ results with $N = 800$ sites. DMRG is unbiased in the sense that neither a spiral nor a BOW phase is assumed. Fig. 7 shows how $ln\xi(x)$ and $ln\lambda(x)$ increase with J_2/J_1. The IQ exponent of $-2/3$ in Eq. (3) fits reasonably well over a smaller range of J_2/J_1 with $c = 3.03$ for λ. The ξ exponent is consistent with the more accurate $c = 2.90$ in Fig. 5 for $B(x)$ and $\Delta(x)$ over a wider range. The scaling form of $\xi(x)$ in the BOW phase and $\lambda(x)$ in the spiral phase are almost identical. According to Eq. (7), the product $\lambda(x)B(x)$ or of $\lambda(x)\Delta(x)$ should be constant, independent of x for large J_2/J_1. The calculated points in Figs. 5 and 7 between $J_2/J_1 = 1.3$ and 3.0 yield $\lambda(x)B(x) \approx 9 \pm 3$ and $\lambda(x)\Delta(x) \approx 5.6 \pm 2$. Since neither is monotonic in J_2/J_1, our results are weakly consistent with constant $\lambda(x)/\xi(x)$. Higher accuracy is needed to test Eq. (7).

The spiral phase of $H(x)$ has been modeled [9–11] in terms of the twist angle $\chi > 0$ for AF exchange that is defined below Eq. (2) for classical spins. The inverse relation between $\lambda(x)$ and $\xi(x)$ in Eq. (7) has been proposed [11, 14] for large $\lambda(x)$ or small χ when the discrete nature of the spin chain is irrelevant. It follows that

$$C(2p) \propto cos(2p\theta) = (-1)^p cos(2p\chi),$$
$$C(2p+1) \propto cos[(2p+1)\theta] = -(-1)^p cos(2p\chi). \quad (10)$$

Even and odd $C(p)$ are not quite out of phase in Fig. 6, in agreement with Eq. (10). The nodes of $C(2r)$ occur at $2r\chi = (n + 1/2)\pi$, while those of $C(2r+1)$ are at $(2r+1)\chi = n\pi$. The angle $\chi(x)$ decreases with increasing J_2/J_1 and has been studied by other techniques [9, 11]. Independent evaluation of $\chi(x) = 2\pi/\lambda(x)$ provides a consistency check for direct DMRG results for $\lambda(x)$ in Fig. 6. Such consistency is different from the common scaling of $\xi(x)$ and $\lambda(x)$ discussed above.

Aligia et al. [11] obtained $\chi(x)$ using twisted boundary conditions in Eq. (1) and exact results up to $N = 24$. Bursill et al. [9] presented several approximation schemes for $\chi(x)$, one of which is based on the peak q^* of the structure factor $S(q)$. The spin-1/2 structure factor for a system with periodic boundary conditions is

$$S(q) = \frac{1}{N}\sum_{np} C(p)\exp(iqp) = \frac{3}{4} + \sum_{p=1} 2C(p)cos(qp) \quad (11)$$

where $C(p)$ are spin correlation functions in Eq. (6). Inversion symmetry is restored in a BOW phase by taking

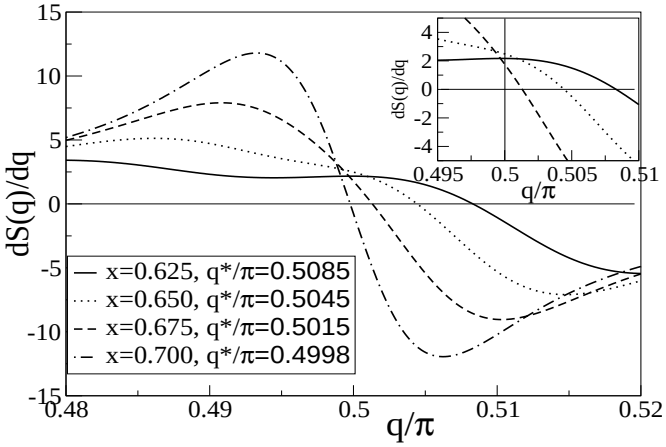

FIG. 8: Derivative $S'(q)$ of the structure factor. The inset shows $S(q^*) = 0$ for $x = 0.625$, 0.65 and 0.675. The twist angle χ is $q^* - \pi/2$ in radians. The $x = 0.700$ result is unphysical.

a linear combination of the degenerate gs. The MG point at $x = 1/3$ has short-range correlations, known exactly, leading to $S_{MG}(q) = 3(1-cosq)/4$ and a broad maximum at $q^* = \pi$. The maximum value $S(q^*)$ is obtained using the derivative

$$\frac{\partial S(q)}{\partial q} = \sum_{p=1} 2pC(p)sin(qp). \qquad (12)$$

Eq. (12) shows that q^* is sensitive to long-range spin correlation functions. We again use $C(p)$ from the central part of the chain. $C(p)$ refers to $n = N/2 = 400$ in Eq. (6) and the sum is from $p = 1$ to $N/2-10$, or 10 sites from chain end. The resulting $S'(q)$ are shown in Fig. 8. The inset magnifies the $S'(q^*) = 0$ region for the indicated values of x. As $\xi(x)$ increases and correlations become long ranged, large p must be retained in the sum and the inherent $1/N$ limitations of OBC are again encountered. Although $q^* = \pi/2 + \chi(x) \to \pi/2$ with increasing x as expected, the condition $S'(q^*) = 0$ has limited value in the crucial region of small χ. The point $q^* = \pi/2$ occurs at $J_1 = 0$ that separates the AF regime with $J_1 > 0$ and $q^* > \pi/2$ from the F regime with $J_1 < 0$ and $q^* < \pi/2$. We underestimate q^* for $x = 0.70$, which is clearly unphysical, and hence overestimate λ based on $S(q)$, but the twist angle and wavelength are consistent for $x < 0.65$.

Aligia et al. [11] emphasize that twisted boundary conditions extend $\chi(x)$ to much larger $J_2/J_1 \approx 30$. They report reasonable agreement with WA [14] and with Bursill et al. [9] up to $J_2/J_1 = 2.5$, where our results are similar. But $\lambda(0.8) \approx 1300$ estimated from $J_2/J_1 = 4$ in their Fig. 4 is about 7 times smaller than the extrapolation of $\lambda(x)$ in Fig. 7. Moreover, their [11] asymptotic regime starts at $J_2/J_1 = 15$ where their $\xi(x)$ has the WA form with exponent -1 in Eq. (3). The stronger presumed decrease of $1/\xi(x)$ in the spiral phase as $x \to 1$ would lose out to the weaker singularity of the BOW phase. Twisted boundary conditions up to $N \approx 24$ do not to give reliable [11] $\Delta(x)$, however, and no $B(x)$ results were presented.

IV. DISCUSSION

We obtained more accurate results for the frustrated spin chain $H(x)$ in Eq. (1) with $J_2/J_1 > 1$ by modifying the DMRG algorithm to add four sites per step instead of two. The order parameter $B(x)$ in Eq. (4) is limited by $1/N$ corrections in systems with open boundary conditions (OBC). The accuracy of the magnetic gap $\Delta(x)$ to the lowest triplet is estimated by comparison to exact results in the fluid phase with $x < x_c = 0.1943$. As seen in Fig. 5, we find an exponential decrease of $B(x)$ and $\Delta(x)$ up to $J_2/J_1 = 4$ that follows the IQ [15] correlation function in Eq. (3) for almost two decades. DMRG automatically yields the spin correlation functions $C(p)$ in Eq. (6) and a spiral phase with wavelength $\lambda(x)$ in Fig. 6. Following WA [14], the correlation length $\xi(x)$ is extracted from amplitudes in the spiral phase. Exponentially increasing $\lambda(x)$ and $\xi(x)$ in Fig. 7 again follows the IQ expression in Eq. (3), albeit over a narrower range up to $x = 0.75(J_2/J_1 = 3)$ set by numerical considerations. The maximum q^* of the structure factor in Fig. 8 is an independent estimate of twist angle $\chi(x) = 2\pi/\lambda(x)$ of the spiral phase in Eq. (2). We find that q^* has limited accuracy for our $C(p)$ for $x > 0.65$.

Detailed comparison with theory is made possible by multiple studies of the BOW [14, 15] and spiral [9, 11] phases of $H(x)$ with $J_2/J_1 > 1$. More generally, we wondered whether DMRG is capable of confirming the small gaps or long correlation lengths predicted by field theory. Our results to $J_2/J_1 = 4$ clearly favor the IQ expression [15] for $\xi(x)$ in Eq. (3) while just as clearly ruling out their fit [15] for $\Delta(x)$. Greater accuracy is needed for meaningful comparisons. The modified algorithm yields multiple and reasonably consistent comparisons up to $J_2/J_1 = 4$.

The modified algorithm runs smoothly for $J_2 > 0$ and $J_1 < 0$. The IQ expression for $\xi(x)$ in Eq. (3) does not depend on the sign of J_1. We find finite gaps Δ on the F side that, however, are less than our estimated numerical accuracy. Still higher accuracy is needed for Δ on the F side. We can definitely say, however, that the constant $c \approx 2.9$ for $\xi(x)$ on the AF side is different from that on the F side. In view of small Δ, Itoi and Qin discuss [15] the spin wave velocity of the singlet or triplet and present conventional DMRG results for $N\Delta$ vs. $1/N$ in Figs. 3 and 4 of Ref. 15. The appearance of a nonsinglet gs at $J_1 \approx -2J_2$ contradicts the exact result of Dmitriev et al. [12], that the singlet/ferromagnetic phase boundary of the zigzag chain is at $J_1 = -4J_2$. Field theory on the

F side is numerically untested so far.

DMRG accounts naturally for coexisting BOW and spiral phases with onsets at $x_c = 0.1943$ and $x_{MG} = 1/3$, respectively, but cannot say where they terminate. Bosonization field theories [14, 15] have a BOW phase but not a spiral phase, while field theory [10] or other approaches [9, 11] to the spiral phase do not yield a BOW. Eq. (7) is an assumed [11, 14] relation between the twist angle $\chi(x)$ of the spiral phase and the correlation length $\xi(x)$ of the BOW phase. The scaling of $\lambda(x)$ and $\xi(x)$ in Fig. 7 is almost the same, and the products $\lambda(x)B(x)$ and $\lambda(x)\Delta(x)$ are roughly constant, but greater accuracy is needed to confirm that $\lambda(x)$ and $\xi(x)$ are indeed proportional. It may be interesting in the future to study whether similar scaling is special to spin-1/2 or holds also for higher spin.

Field theory is a continuum approximation. Since solid-state models are discrete, field theory becomes accurate when $\xi(x)$ exceeds 5-10 lattice constants. This is well documented for solitons in the SSH model [23] and its continuum version [24]. As shown in Fig. 7, $\xi(x) > 10$ requires $J_2/J_1 > 1$ and our DMRG extends to $\xi \approx 300$. We do not consider the discreteness of the lattice to be important.

It is a well-recognized numerical challenge, to obtain exponentially small energy gaps or exponentially long correlation lengths near a quantum phase transition. Impressive gains in numerical accuracy are required to be modestly closer to the critical point. The modified DMRG algorithm for $H(x)$ extends accurate results to $J_2/J_1 = 4$ and clearly favors the correlation function $\xi(x)$ in Eq. (3) proposed by Itoi and Qin [15]. There are open questions such as whether $J_2/J_1 = 4$ is in the asymptotic limit or the relation between BOW and spiral phases. Convincing comparison between field theory and numerical methods are in fact demanding as we have illustrated for the zigzag spin-1/2 chain.

Acknowledgments. We gratefully acknowledge partial support for work at Princeton by the National Science Foundation under the MRSEC program (DMR-0819860). SR thanks DST India for funding through SR/S1/IC-08/2008 and JC Bose fellowship.

[1] D. C. Johnston, R. K. Kremer, M. Troyer, X. Wang, A. Klumpfer, S. L. Bud'ko, A. F. Panchula and P. C. Canfield, Phys. Rev. B **61**, 9558 (2000), and references therein.
[2] H. Bethe, Z. Phys. **71**, 205 (1931).
[3] L. Hulthen, Arkiv. Mat. Astron. Fysik. **26A**, No. 11 (1938).
[4] C. K. Majumdar and D. K. Ghosh, J. Math. Phys. **10**, 1399 (1969).
[5] F. D. M. Haldane, Phys. Rev. B **25**, 4925 (1982).
[6] K. Kuboki and H. Fukuyama, J. Phys. Soc. Japan **56**, 3126 (1987).
[7] I. Affleck, D. Gepner, H. J. Schultz and T. Ziman, J. Phys. A **22**, 511 (1989).
[8] K. Okamoto and K. Nomura, Phys. Lett. A **169**, 433 (1992).
[9] R. Bursill, G. A. Gehring, D. J. J. Farnell, J. B. Parkinson, T. Xiang and C. Zeng, J. Phys: Condens. Matter **7**, 8605 (1995).
[10] S. Rao and D. Sen, Nucl. Phys. B **424**, 547 (1994); S. Allen and D. Senechal, Phys. Rev. B **51**, 6394 (1995).
[11] A. A. Aligia, C. D. Batista and F. H. L. Essler, Phys. Rev. B **62**, 3259 (2000).
[12] D. V. Dmitriev, V. Ya. Krivnov and A. A. Ovchinnikov, Phys. Rev. B **56**, 5985 (1997).
[13] M. Hase, H. Kuroe, K. Ozawa, O. Suzuki, H. Kitazawa, G. Kido and T. Sekine, Phys. Rev. B **70**, 104426 (2004).
[14] S. R. White and I. Affleck, Phys. Rev. B **54**, 9862 (1996).
[15] C. Itoi and S. Qin, Phys. Rev. B **63**, 224423 (2001).
[16] M. Kumar, Z. G. Soos and S. Ramasesha, Phys. Rev. B (in press).
[17] T. Tonegawa and I. Harada, J. Phys. Soc. Japan **56**, 2153 (1987); R. Chitra, S. Pati, H. R. Krishnamurthy, D. Sen and S. Ramasesha, Phys. Rev. B **52**, 6581 (1995).
[18] S. R. White, Phys. Rev. Lett. **69**, 2863 (1992).
[19] S. R. White, Phys. Rev. B **48**, 10345 (1993)
[20] U. Schollwöck, Rev. Mod. Phys. **77**, 259 (2005)
[21] K. Hallberg, New Trends in Density Matrix Renormalization, Advances in Phys. **55**, 477 (2006).
[22] C. A. Coulson, Proc. R. Soc. London, A **169**, 413 (1939); Z. G. Soos, S. Ramasesha, D. S. Galvao and S. Etemad, Phys. Rev. B **47**, 1742 (1993).
[23] W. P. Su, J. R. Schrieffer and A. J. Heeger, Phys. Rev. Lett. **44**, 1698 (1979); Phys. Rev. B **22**, 2099 (1980).
[24] H. Takayama, Y.R. Lin-Liu and K. Maki, Phys. Rev. B **21**, 2388 (1980).